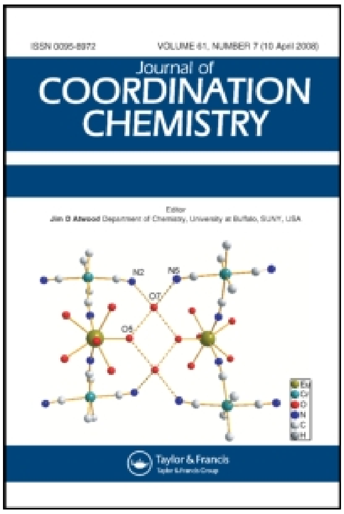

Journal of Coordination Chemistry
Publication details, including instructions for authors and subscription information:
http://www.informaworld.com/smpp/title~content=t713455674

Syntheses and crystal structures of cobalt and nickel complexes of 2,6-bis(hydroxymethyl)pyridine

Silke Winter[a]; Wilhelm Seichter[a]; Edwin Weber[a]
[a] Institut für Organische Chemie, Technische Universität Bergakademie Freiberg, D-09596 Freiberg/Sachsen, Germany

To cite this Article Winter, Silke , Seichter, Wilhelm and Weber, Edwin(2004) 'Syntheses and crystal structures of cobalt and nickel complexes of 2,6-bis(hydroxymethyl)pyridine', Journal of Coordination Chemistry, 57: 12, 997 — 1014
To link to this Article: DOI: 10.1080/00958970412331272395
URL: http://dx.doi.org/10.1080/00958970412331272395

J. Coord. Chem., Vol. 57, No. 12, 15 August 2004, pp. 997–1014

Taylor & Francis
Taylor & Francis Group

SYNTHESES AND CRYSTAL STRUCTURES OF COBALT AND NICKEL COMPLEXES OF 2,6-BIS(HYDROXYMETHYL)PYRIDINE

SILKE WINTER, WILHELM SEICHTER and EDWIN WEBER*

Institut für Organische Chemie, Technische Universität Bergakademie Freiberg, Leipziger Str. 29, D-09596 Freiberg/Sachsen, Germany

(Received 3 February 2004)

2 : 1 (L : M) Complexes of 2,6-bis(hydroxymethyl)pyridine (dhmp) with different Co(II) salts [$CoCl_2 \cdot 6H_2O$, $Co(SCN)_2$, $Co(NO_3)_2 \cdot 6H_2O$, $CoSO_4 \cdot 7H_2O$ and $Co(OTos)_2 \cdot 6H_2O$] and Ni(II) salts [$NiCl_2 \cdot 6H_2O$, $Ni(NO_3)_2 \cdot 6H_2O$, $NiSO_4 \cdot 7H_2O$ and $Ni(OTos)_2 \cdot 6H_2O$] have been prepared (**1**–**9**) and studied by infrared spectroscopy and X-ray crystallography. Influences on the distortion of the coordination polyhedron, the arrangement of the donor atoms and the packing structure of the complexes were investigated in terms of the different kinds of anions and cations. In the metal chloride Complexes **1** and **2**, water of hydration was found, while in Complex **3** the counterion (SCN^-) acts as a ligand. The crystal structures of all complexes, except **3**, show N_2O_4 hexacoordinated metal ions; in **3** the coordination environment is N_4O_2. Complex **1** is another exception in containing cobalt(III) instead of cobalt(II) as for the other complexes with cobalt salts. Logically, in Complex **1**, one of the dhmp ligands is mono-deprotonated. In the neutral Complexes **2** and **4**–**9**, the basal planes of the octahedra are made up of O donors and N atoms occupy the axial positions. In **1** as well as in **3**, two N and two O atoms form the base, but in **1** O, and in **3** N atoms are on the axis of the coordination sphere. Moreover, the nickel Complexes **2**, **5**, **7** and **9** are more symmetrical in structure than the cobalt Complexes **1**, **4**, **6** and **8**, in accordance with the Jahn–Teller effect. Packing structures of the complexes show specific interactions based on strong and weak H-bonds that involve the counterions, hydroxy groups and aromatic units, leading to extended network structures.

Keywords: 2,6-Disubstituted pyridine; Cobalt complexes; Nickel complexes; Synthesis; Crystal structure

INTRODUCTION

Pyridines have been extensively investigated as ligands in coordination compounds [1]. Recently, useful coordination polymers increasingly benefit from pyridine units that coordinate to different metal centers [2]. Moreover, 2,6-disubstituted pyridines show the ability to act as chelating ligands [3]. A characteristic representative is 2,6-bis(hydroxymethyl)pyridine (dhmp = LH_2, Fig. 1), which forms complexes with Pt as a monodentate ligand [4], with Tc(V) as a bidentate partially deprotonated ligand [5] and with Hg [6] and Cu(II) [7,8] as a tridentate ligand.

---

*Corresponding author. E-mail: edwin.weber@chemie.tu-freiberg.de

ISSN 0095-8972 print: ISSN 1029-0389 online © 2004 Taylor & Francis Ltd
DOI: 10.1080/00958970412331272395

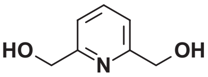

LH_2 (dhmp)

1: $[Co(LH_2)LH]Cl_2\cdot H_2O$

2: $[Ni(LH_2)_2]Cl_2\cdot 0.5H_2O$

3: $[Co(LH_2)_2(NCS)_2]$

4: $[Co(LH_2)_2](NO_3)_2$

5: $[Ni(LH_2)_2](NO_3)_2$

6: $[Co(LH_2)_2]SO_4$

7: $[Ni(LH_2)_2]SO_4$

8: $[Co(LH_2)_2](OTos)_2$

9: $[Ni(LH_2)_2](OTos)_2$

FIGURE 1 Compounds studied in this paper.

In a preliminary study aimed at the design of new building blocks for coordination polymers based on dhmp as the active component, complexes of dhmp with different salts of Cu(II) were investigated; this supplied information about potential anion competition in these complexes [8]. In the present paper, we have studied further the coordination behavior of dhmp with different cations, including the potential participation of anions in the coordination. We report here the preparation and structural characterization of complexes formed by dhmp with different salts of Co(II) and Ni(II) [$CoCl_2\cdot 6H_2O$, $Co(SCN)_2$, $Co(NO_3)_2\cdot 6H_2O$, $CoSO_4\cdot 7H_2O$, $Co(OTos)_2\cdot 6H_2O$, $NiCl_2\cdot 6H_2O$, $Ni(NO_3)_2\cdot 6H_2O$, $NiSO_4\cdot 7H_2O$, and $Ni(OTos)_2\cdot 6H_2O$], including IR spectra and X-ray crystallographic structures.

EXPERIMENTAL

The starting compound dhmp and the metal salts were obtained from the usual suppliers (Aldrich, Merck-Schuchardt, Fluka). Elemental analyses were performed on a Heraeus CHN instrument. Infrared spectra (KBr pellets) were recorded on a Nicolet 510 spectrophotometer (400–4000 cm^{-1}).

Preparation of the Co(II) and Ni(II) Tosylates

Some 88 mmol of the respective metal(II) chloride hexahydrate ($CoCl_2\cdot 6H_2O$, $NiCl_2\cdot 6H_2O$) were dissolved in 70 cm^3 of water, and 176 cm^3 of aqueous 1 M NaOH were added. The precipitated hydroxide was collected and washed with water. Then, 8 g (46.7 mmol) of *p*-toluenesulfonic acid was dissolved in 200 cm^3 of water, and an excess of the hydroxide was added. The mixture was refluxed until most of the hydroxide had dissolved. Excess metal hydroxide was filtered off and the solution concentrated. On cooling, the metal(II) tosylate hexahydrate crystallized. The isolated crude product was recrystallized from ethanol.

$Co(OTos)_2 \cdot 6H_2O$: 81% yield of pink crystals. Anal. Calcd. for $C_{14}H_{14}CoO_6S_2 \cdot 6H_2O$(%): C, 33.01; H, 5.14. Found: C, 33.00; H, 5.17. IR spectra: $\nu_s(SO_3)$ salt of aromatic sulfonic acid, 1126, 1040 1013, vs. $Ni(OTos)_2 \cdot 6H_2O$: 67% yield of light green crystals. Anal. Calcd. for $C_{14}H_{14}NiO_6S_2 \cdot 6H_2O$(%): C, 33.02; H, 5.15. Found: C, 33.06; H, 5.19. IR spectra: $\nu_s(SO_3)$ salt of aromatic sulfonic acid, 1126, 1040 1013, vs.

Preparation of the Complexes

All complexes were prepared under atmospheric conditions. Some 7 mmol of dhmp and 3.5 mmol of the respective metal salt were dissolved in 30 to 50 cm^3 of ethanol (in case of the chlorides 10 cm^3 of water was added to achieve better solubility of the salts) and refluxed for 1 h. The solvent was removed under reduced pressure, and the residue was recrystallized from a little water. Crystals were collected and washed with small portions of cold water and cold methanol. Yields, melting points and analytical data are given in Table I.

Crystal Structure Determination

Intensity data, collected on a CAD4 diffractometer (graphite-monochromated Cu Kα radiation), were measured in the ω–2θ scan mode. Cell constants and orientation matrices were refined by least-squares fits of 25 reflections. Three standard reflections measured after every hour showed no decay of the crystal during the data collections. Reflections were corrected for background, Lorentz and polarization effects. The crystal structures were solved by direct methods [9] and difference Fourier syntheses, and refined by full-matrix least-squares procedures [10]. Absorption corrections were performed by using the WinGX program [11]. All nonhydrogen atoms were refined anisotropically. Hydrogen atoms of the hydroxyl groups were partly obtained from difference Fourier maps, but in other cases were included in the models in calculated positions, and then refined as being constrained to bonding atoms.

Supplementary material for the crystal structure determinations has been deposited at the Cambridge Crystallographic Data Centre and can be ordered under CCDC

TABLE I Analytical data, melting points and percentage yields for complexes

Complex	*Color*	*Found (Calculated)%*			*Mp* (°C)	*Yield* (%)
		C	*H*	*N*		
$[Co(LH_2)LH]Cl_2 \cdot H_2O$ (**1**)	lilac	41.33 (41.20)	4.80 (4.45)	6.86 (6.86)	151 dec.	28
$[Ni(LH_2)_2]Cl_2 \cdot 0.5H_2O$ (**2**)	green	41.09 (41.22)	4.65 (4.45)	6.92 (6.87)	276 dec.	30
$[Co(LH_2)_2(NCS)_2]$ (**3**)	lilac	42.42 (42.39)	4.05 (4.00)	11.94 (12.36)	179	54
$[Co(LH_2)_2](NO_3)_2$ (**4**)	lilac	36.39 (36.46)	3.87 (3.93)	11.98 (12.15)	197 dec.	25
$[Ni(LH_2)_2](NO_3)_2$ (**5**)	green	36.59 (36.48)	3.91 (3.94)	11.86 (12.15)	200 dec.	32
$[Co(LH_2)_2]SO_4$ (**6**)	lilac	37.44 (37.27)	4.05 (4.47)	6.11 (6.21)	280 dec.	20
$[Ni(LH_2)_2]SO_4$ (**7**)	blue–green	38.86 (38.83)	4.33 (4.19)	6.41 (6.47)	>360	48
$[Co(LH_2)_2](OTos)_2$ (**8**)	lilac	49.60 (49.48)	4.83 (4.75)	4.12 (4.12)	263	62
$[Ni(LH_2)_2](OTos)_2$ (**9**)	blue	49.67 (49.50)	4.80 (4.75)	4.19 (4.12)	290	78

Nos. 224884 (**1**), 224886 (**2**), 224890 (**3**), 224885 (**4**), 224888 (**5**), 224887 (**6**), 224891 (**7**), 224892 (**8**) and 224889 (**9**).

RESULTS AND DISCUSSION

All chelate Complexes **1**–**9** (Fig. 1) were prepared by co-crystallization of stoichiometric amounts of dhmp and the respective Co(II) and Ni(II) salts from an ethanolic solution.

Infrared Spectra

Infrared data and band assignments for the different chelate complexes including uncomplexed dhmp are listed in Table II. Free dhmp has major peaks at 3363, 2778, 1600, 1577, 1471, 1411 and 1084 cm^{-1}. Strong bands at 3363 and 2778 cm^{-1} are assigned to O–H stretching. Bands in the region 1600–1471 cm^{-1} are assigned to ring vibrations, those at 1084 cm^{-1} to C–O stretching, and those at 1411 cm^{-1} to in-plane C–OH deformation.

TABLE II Characteristic IR frequencies (cm^{-1}) and assignments for 2,6-bis(hydroxymethyl)pyridine (dhmp) and its Co and Ni complexes **1**–**9**

	$\nu(OH)$	$\nu(ring)$	$\delta_{ip}(C\text{–}OH)$	$\nu(C\text{–}O)$
LH_2 (dhmp)	3363 2778	1600 1577 1471	1411	1084
$[Co(LH_2)LH]Cl_2 \cdot H_2O$ (**1**)	3410 m, br 3074 vs, br	1612 m-s 1850 1478	1292 s	1041–1024 vs
$[Ni(LH_2)_2]Cl_2 \cdot 0.5H_2O$ (**2**)	3425 vs, br 3080 vs, br	1606 s 1583 1473	1298 m	1034–1023 vs
$[Co(LH_2)_2(NCS)_2]$ (**3**)[a]	3224 vs 3110 s	1602 s 1574 1461	1399 m 1229 m	1052 vs
$[Co(LH_2)_2](NO_3)_2$ (**4**)	3076 s, br	1608 m 1583 1475	1334 s	1032–1021 s
$[Ni(LH_2)_2](NO_3)_2$ (**5**)	3084 vs, br	1609 m-s 1583 1476	1291 m	1038–1015 s
$[Co(LH_2)_2]SO_4$ (**6**)	3074 vs	1609 m-s 1581 1476	1291 s	1034–1017 vs
$[Ni(LH_2)_2]SO_4$ (**7**)	3056 s	1608 m 1584 1482	1345 m	1020 vs
$[Co(LH_2)_2](OTos)_2$ (**8**)	3072 vs, br	1608 w-s 1582 1476	1290 m	1033 vs 1014 vs
$[Ni(LH_2)_2](OTos)_2$ (**9**)	3076 vs, br	1610 w-s 1584 1477	1290 m	1038 vs

vs, very strong (90–100%); s, strong (60–90%); m, medium (30–60%); w, weak (10–30%), br, broad.

[a] Additional band at 800 cm^{-1} due to ν(C–S).

With reference to free dhmp, the chelate complexes show characteristic features. OH stretching appears as a broad band with maxima at 3074 and 3410 cm^{-1} in the hydrated Complex **1**, and at 3080 and 3425 cm^{-1} in **2**. Also, in Complex **3**, we observe two bands with maxima at 3110 and 3224 cm^{-1}, indicating that one OH group is involved in a strong H bridge while the other forms an intramolecular chelate bridge. In the other complexes (**4**–**9**), single bands ranging between 3056 and 3085 cm^{-1} were found. The 1600 cm^{-1} absorption of the pyridine ring in free dhmp is shifted to higher values (1602–1612 cm^{-1}) in the complexes due to coordination of the pyridine nitrogen to the metal ion. Moreover, 1411 and 1084 cm^{-1} absorptions of free dhmp are shifted to 1290 and 1038–1013 cm^{-1} in the complexes as a result of coordination. A band at 800 cm^{-1} in Complex **3**, assigned to C–S stretching, indicates nitrogen-bonded SCN.

Crystal Structures of the Complexes

Crystals of the Complexes **1**–**9** for X-ray determinations were grown by slow evaporation of solvent from solutions in water/ethanol. Details of data collection and refinement procedures are given in Table III. Structural parameters of selected interactions are listed in Tables IV and V. In order to make a better comparison, description of the complexes is arranged according to the counterion.

Crystal Structures of $[Co(LH_2)LH]Cl_2 \cdot H_2O$ (1) and $[Ni(LH_2)_2]Cl_2 \cdot 0.5H_2O$ (2)

Unexpectedly, crystallization of cobalt(II) chloride hexahydrate with dhmp yields a complex (**1**) that contains Co(III) and one water molecule per formula unit (Fig. 2). Obviously, Co(II) has been oxidized to Co(III) under the given conditions (air and room temperature) and is stabilized through complexation. The oxidation state of cobalt has been confirmed by an EPR measurement indicating that **1** is low spin. Thus, one OH group of dhmp in the complex cation is deprotonated. In this complex, the coordination environment around the cobalt ion is a strongly distorted octahedron (CoN_2O_4) with pyridine nitrogens and two oxygens of the mono-deprotonated dhmp (LH) in basal and the OH groups of neutral dhmp in axial positions. The complex geometry can be explained by the rigid ligand structure resulting in N–Co–N and O–Co–O bond angles that deviate significantly from linearity (see Table IV). The Co–O distance of the ionized oxygen is shorter (1.995 Å) than the other Co–O bond lengths, which range between 2.157 and 2.171 Å. The Co–N distances of 2.02 and 2.04 Å are in the same range as found for analogous copper(II) complexes [8]. The O–H groups are hydrogen bonded to the chloride anions and the water molecule with H···Cl bond distances of 2.109 and 2.137 Å and a short O···H contact of 1.661 Å (Table V).

As shown in the packing of **1** (Fig. 3), binding modes of the chloride anions are different. One chloride ion bridges two complex cations whereas the other, together with the water molecule, forms infinite hydrogen-bonded helical strands that run along the *b* axis.

Similarly to **1**, the nickel(II) complex also crystallizes in a hydrated form. However, differences regarding water content as well as lattice constants suggest structural differences between the two complexes. Unlike **1**, in the nickel complex **2** the water molecules are not associated with the complex cation units, but are incorporated into the domains of the chloride ions, as illustrated in Fig. 4. Although the positions of the water hydrogens could not be identified during structure refinement, Cl–O distances (3.3 Å)

TABLE III Crystal data and structure refinement details for the Complexes **1–9**

	1	***2***	***3***	***4***	***5***	***6***	***7***	***8***	***9***
Empirical Formula	$C_{14}H_{19}N_2O_5Cl_2Co$	$C_{14}H_{19}N_2O_{4.5}Cl_2$ Ni	$C_{16}H_{18}N_4O_4S_2Co$	$C_{14}H_{18}N_4O_{10}Co$	$C_{14}H_{18}N_4O_{10}Ni$	$C_{14}H_{18}N_2O_8SCo$	$C_{14}H_{18}N_2O_8SNi$	$C_{28}H_{32}N_2O_{10}S_2Co$	$C_{28}H_{32}N_2O_{10}S_2Ni$
Formula weight	425.14	417.93	453.39	461.25	461.01	433.29	433.07	679.61	679.38
Temperature/K	298(2)	296(2)	298(2)	298(2)	293(2)	178(2)	294(2)	298(2)	294(2)
Wavelength λ/Å	1.5418	1.5418	1.5418	1.5418	1.5418	1.5418	1.5418	1.5418	1.5418
Crystal system	monoclinic	monoclinic	monoclinic	triclinic	triclinic	monoclinic	triclinic	triclinic	triclinic
Space group	$C2/c$	$P2_1/a$	$P2_1/c$	P-1	P-1	$C2/c$	P-1	P-1	P-1
a/Å	28.849(6)	13.202(2)	16.716(3)	7.452(1)	8.320(3)	27.397(4)	7.009(1)	10.033(2)	7.920(1)
b/Å	8.217(2)	9.210(1)	12.684(3)	9.922(2)	10.046(5)	8.254(1)	8.167(2)	10.529(2)	11.508(2)
c/Å	18.962(4)	16.376(3)	9.233(2)	13.413(3)	11.525(3)	15.950(2)	14.784(3)	14.805(3)	17.335(5)
$\alpha/^\circ$	90.0	90.0	90.0	90.96(3)	84.37(3)	90.0	75.78(3)	105.16(3)	94.81(1)
$\beta/^\circ$	129.30(3)	113.76(1)	89.97(3)	105.25(3)	74.82(3)	107.11(1)	81.24(3)	95.63(3)	98.42(1)
$\gamma/^\circ$	90.0	90.0	90.0	106.00(3)	71.23(3)	90.0	86.51(3)	94.81(3)	104.82(1)
V/Å^3	3478.4(13)	1822.4(5)	1957.6(7)	915.5(3)	880.1(6)	3447.2(8)	810.5(3)	1492.5(5)	1498.7(5)
Z	8	4	4	2	2	8	2	2	2
$D_{calc}/g\,cm^{-3}$	1.624	1.523	1.538	1.673	1.679	1.670	1.774	1.512	1.492
μ/mm^{-1}	10.813	4.439	9.133	7.95	2.149	9.380	3.400	6.334	2.752
$F(000)$	1744	864	932	474	460	1784	448	706	696
Reflect. coll.	3588	3546	3333	3768	3618	3539	3289	6144	5852
Reflect. obs. $[I > 2\sigma(I)]$	2379	2732	1966	2948	3169	2486	2846	4070	4513
Parameters	233	216	244	275	257	251	239	402	423
$R[I > 2\sigma(I)]$	0.0736	0.0606	0.0941	0.0828	0.0594	0.0670	0.0503	0.0650	0.0771
ωR	0.1702	0.1709	0.2559	0.2082	0.1605	0.1600	0.1329	0.1604	0.2040
Goodness-of-fit	1.062	0.987	0.994	1.092	1.162	1.047	1.177	0.906	1.121
Peak/hole/e Å^{-3}	0.67/−1.05	1.23/−0.39	0.97/−0.77	1.29/−1.35	0.59/−0.60	1.24/−0.96	1.09/−0.56	0.64/−0.55	1.29/−1.35

TABLE IV Selected bond lengths (Å) and angles (°) for the Complexes **1**–**9**

	1	**3**	**4**	***6***	***8***		**2**	**5**	***7***	***9***
Bond lengths										
Co(1)–O(1)	2.157(5)	2.106(6)	2.112(4)	2.161(4)	2.133(4)	Ni(1)–O(1)	2.115(3)	2.132(3)	2.106(2)	2.080(4)
Co(1)–O(2)	1.995(4)		2.136(4)	2.139(5)	2.127(4)	Ni(1)–O(2)	2.094(3)	2.119(3)	2.117(2)	2.091(4)
Co(1)–O(3)	2.171(5)	2.099(6)	2.100(4)	2.152(4)	2.129(4)	Ni(1)–O(3)	2.091(3)	2.051(2)	2.151(2)	2.076(4)
Co(1)–O(4)	2.166(5)		2.124(4)	2.137(4)	2.106(4)	Ni(1)–O(4)	2.115(3)	2.121(2)	2.106(2)	2.092(4)
Co(1)–N(1)	2.021(5)	2.211(7)	2.033(4)	2.043(4)	2.043(4)	Ni(1)–N(1)	1.971(3)	1.982(3)	1.994(3)	1.983(4)
Co(1)–N(2)	2.044(5)	2.207(8)	2.048(4)	2.047(4)	2.048(4)	Ni(1)–N(2)	1.968(3)	1.970(3)	1.980(3)	1.974(4)
Co(1)–N(3)		2.041(8)								
Co(1)–N(4)		2.061(9)								
Bond angles										
N(1)–Co(1)–N(2)	163.9(2)	151.3(3)	164.1(2)	162.0(2)	166.9(2)	N(1)–Ni(1)–N(2)	179.4(2)	177.1(1)	172.3(1)	171.1(2)
O(1)–Co(1)–O(2)	152.3(2)		147.5(2)	148.6(2)	153.2(2)	O(3)–Ni(1)–O(4)	156.2(1)	156.5(1)	155.4(1)	156.3(2)
O(3)–Co(1)–O(4)	152.0(2)		149.4(2)	148.9(1)	147.4(2)	O(1)–Ni(1)–O(2)	156.2(1)	158.5(1)	155.8(1)	156.5(2)
O(1)–Co(1)–O(3)		92.6(3)								
O(1)–Co(1)–N(4)		174.1(3)								
N(2)–Co(1)–N(3)		109.4(3)								
N(1)–Co(1)–N(4)		109.3(3)								
N(3)–Co(1)–N(4)		92.5(3)								
Torsion angles										
N(1)–C(5)–C(7)–O(2)	−7.1(8)	172.0(8)	4.7(6)	6.1(8)	−15.7(7)	N(1)–C(5)–C(7)–O(2)	−19.5(5)	8.7(6)	10.2(4)	13.5(7)
N(1)–C(1)–C(6)–O(1)	−10.0(8)	−22.2(12)	10.1(7)	−11.0(6)	2.6(8)	N(1)–C(1)–C(6)–O(1)	−8.1(5)	−5.0(5)	−0.4(4)	−4.1(7)
N(2)–C(8)–C(13)–O(3)	−16.2(7)	−23.2(12)	14.5(7)	−18.1(7)	5.6(6)	N(2)–C(8)–C(13)–O(3)	−19.1(5)	0.5(4)	16.9(4)	10.8(7)
N(2)–C(12)–C(14)–O(4)	−10.8(8)	174.0(8)	2.7(7)	1.5(8)	−6.7(7)	N(2)–C(12)–C(14)–O(4)	−7.3(5)	−13.8(5)	20.0(4)	3.5(9)

TABLE V Selected hydrogen bond interactions in the complexes **1**–**9**

D–H···A	*Symmetry*	*Distances* (Å)		*Angles* (°) *D–H···A*
		D···A	*H···A*	
1				
O(1)–H(1′)···Cl(1)	*x*, −*y* + 1, *z* + 0.5	3.033(5)	2.14	168
O(3)–H(3′)···Cl(2)	*x*, *y*, *z*	3.001(5)	2.11	166
O(4)–H(4′)···O(1W1)	*x*, *y*, *z*	2.608(7)	1.66	171
O(1W1)–H(1W1)···Cl(1)	−*x* + 0.5, −*y*, *z* + 1	3.161(5)	2.25	169
O(1W1)–H(2W1)···Cl(1)	*x*, −*y*, *z* + 1	3.079(5)	2.22	157
2				
O(1)–H(1′)···Cl(2)	*x*, *y*, *z*	3.038(3)	2.22	175
O(2)–H(2′)···Cl(1)	−*x* + 0.5, *y* − 0.5, −*z* + 1	2.992(3)	2.20	164
O(3)–H(3′)···Cl(1)	*x*, *y*, *z*	2.993(3)	2.23	156
O(4)–H(4′)···Cl(2)	−*x*, −*y*, −*z*	3.037(3)	2.22	177
O(1W)···Cl(2)	*x*, *y*, *z*	3.292(3)		
O(1W)···Cl(2)	−*x* + 0.5, *y* + 0.5, −*z*	3.317(3)		
3				
O(1)–H(1′)···O(4)	*x*, −*y* − 0.5, *z* + 0.5	2.630(8)	1.81	178
O(2)–H(2′)···S(2)	*x*, −*y* + 0.5, *z* + 0.5	3.175(8)	2.37	167
O(3)–H(3′)···O(2)	*x*, −*y* + 0.5, *z* + 0.5	2.639(8)	1.82	178
O(4)–H(4′)···S(1)	*x*, −*y* − 0.5, *z* + 0.5	3.196(8)	2.63	128
4				
O(1)–H(1′)···O(5)	*x*, *y*, *z*	2.726(7)	1.78	173
O(2)–H(2′)···O(8)	*x*, *y*, *z*	2.642(6)	1.62	170
O(3)–H(3′)···O(7)	*x* + 1, *y*, *z*	2.606(6)	1.80	172
O(4)–H(4′)···O(9)	−*x* + 1, −*y* + 1, −*z* + 2	2.722(6)	1.94	159
5				
O(1)–H(1′)···O(6)	*x* + 1, *y*, *z*	2.718(4)	1.90	175
O(2)–H(2′)···O(8)	*x*, *y*, *z*	2.779(7)	2.14	135
O(2)–H(2′)···O(9)	*x*, *y*, *z*	2.872(6)	2.15	146
O(3)–H(3′)···O(3)	−*x*, −*y* + 1, −*z* + 2	2.476(6)	1.70	157
O(4)–H(4′)···O(7)	−*x*, −*y*, −*z* + 1	2.661(6)	1.85	168
C(6)–H(6A)···O(5)	*x* − 1, *y*, *z*	3.442(7)	2.65	137
C(6)–H(6B)···O(8)	*x* − 1, *y*, *z*	3.213(7)	2.35	149
6				
O(1)–H(1′)···O(1A)	−*x* + 0.5, *y* + 0.5, −*z* + 0.5	2.598(6)	1.77	169
O(2)–H(2′)···O(4A)	−*x* + 0.5, *y*–0.5, −*z* + 0.5	2.605(6)	1.82	154
O(3)–H(3′)···O(2A)	−*x* + 0.5, *y* + 0.5, −*z* + 0.5	2.559(5)	1.74	164
O(4)–H(4′)···O(3A)	−*x* + 0.5, −*y* + 0.5, −*z*	2.578(6)	1.74	177
C(8)–H(6B)···O(1A)	*x* − 0.5, *y* + 0.5, *z*	3.212(7)	2.58	147
C(11)–H(11)···O(2A)	*x*, *y*, *z*	3.392(6)	2.51	154
C(6)–H(6A)···O(3A)	−*x* + 0.5, −*y* + 0.5, −*z*	3.379(6)	2.60	136
C(13)–H(13A)···O(4A)	−*x* + 0.5, −*y* + 0.5, −*z* + 0.5	3.306(6)	2.43	147
7				
O(1)–H(1′)···O(5)	*x*, *y* + 1, *z*	2.549(3)	1.74	170
O(2)–H(2′)···O(6)	*x* + 1, *y*, *z*	2.575(3)	1.79	159
O(3)–H(3′)···O(8)	*x* + 1, *y* + 1, *z*	2.699(3)	1.89	168
O(4)–H(4′)···O(6)	*x* + 1, *y* + 1, *z*	2.658(3)	1.89	173
C(13)–H(13A)···O(7)	*x* + 1, *y* + 1, *z*	3.200(3)	2.34	148
C(13)–H(13B)···O(5)	*x*, *y* + 1, *z*	3.291(3)	2.50	140
8				
O(1)–H(1′)···O(9)	*x*, *y*, *z*	2.618(5)	1.80	172
O(2)–H(2′)···O(8)	*x*, *y*, *z*	2.613(5)	1.72	176
O(3)–H(3′)···O(7)	*x*, *y*, *z*	2.501(5)	1.73	174
O(4)–H(4′)···O(5)	*x* + 1, *y*, *z*	2.591(5)	1.67	166
9				
O(1)–H(1′)···O(3G1)	−*x* + 1, −*y* + 1, −*z* + 1	2.644(6)	1.83	173
O(2)–H(2′)···O(3G2)	−*x*, −*y* + 1, −*z* + 1	2.583(5)	1.79	163
O(3)–H(3′)···O(1G1)	*x*, *y*, *z* + 1	2.646(5)	1.83	173
O(4)–H(4′)···O(1G2)	−*x* + 1, −*y* + 1, −*z* + 1	2.632(6)	1.81	177

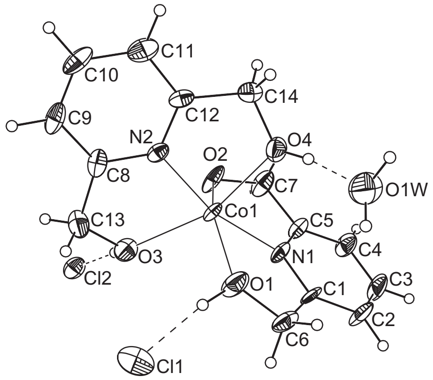

FIGURE 2 Molecular structure of the hydrated complex **1** (50% probability thermal ellipsoids) showing the atom numbering scheme. Bold, thin and broken lines represent covalent, coordination and ordinary H bonds, respectively.

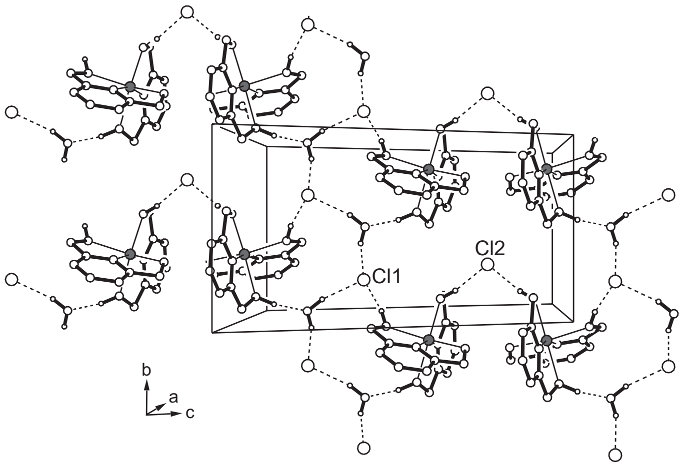

FIGURE 3 Packing structure of Complex **1** indicating the system of H-bonds (broken lines). Nonrelevant hydrogens are omitted for clarity.

and Cl–O–Cl bond angles (119.7°) indicate the presence of hydrogen bonds between water molecules and anions (Table V). Thus a nearly tetrahedral coordination environment of chloride ions occurs, exploiting in a nearly ideal manner the acceptor potential of these anions by hydrogen bonding with four strong donors.

The complex exhibits a packing structure that is characterized by alternating layers of cations (C) and anions (A). As only every second anion layer contains the water molecules, the order of the layers is C–A–C–A′–C. An analogous structure pattern was also found in the related copper(II) complex of dhmp, which, however, is solvent-free [8].

Crystal Structure of [Co(LH$_2$)$_2$(NCS)$_2$] (3)

Crystallization of Co(SCN)$_2$ in the presence of dhmp yields a complex in which the thiocyanate ions (more correctly isothiocyanate ions, because nitrogen atoms are coordinated to the metal) are involved in the coordination sphere of the cobalt ion (Fig. 5).

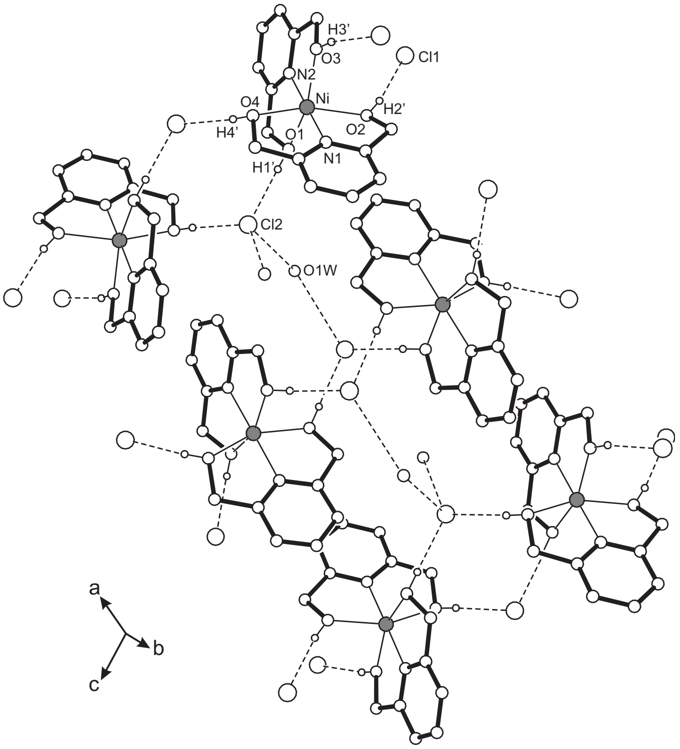

FIGURE 4 Packing structure of the hydrated complex **2**. For clarity, only the hydrogens of the hydroxy groups are shown while the water molecules are represented only by the oxygen atoms; all other hydrogens are omitted.

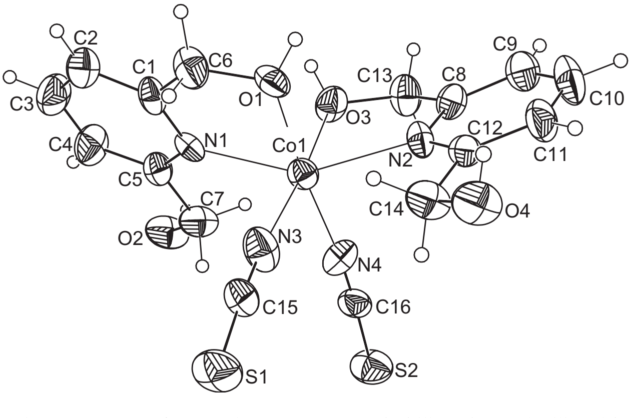

FIGURE 5 Molecular structure of Complex **3** (50% probability thermal ellipsoids) showing the atom numbering scheme. Bold and thin lines represent covalent and coordination bonds, respectively.

Thus a more regular, less strained coordination polyhedron results with the anions in *syn* positions (N3–Co–N4 91.2°). The distances within the basal plane are 2.100 and 2.107 Å for the Co–O bonds, and 2.035 and 2.047 Å for the Co–N bonds, whereas the pyridine nitrogens, which occupy axial positions, show Co–N distances of 2.207 Å (Table IV). Due to coordination of the cobalt ion, two functional groups of the complex

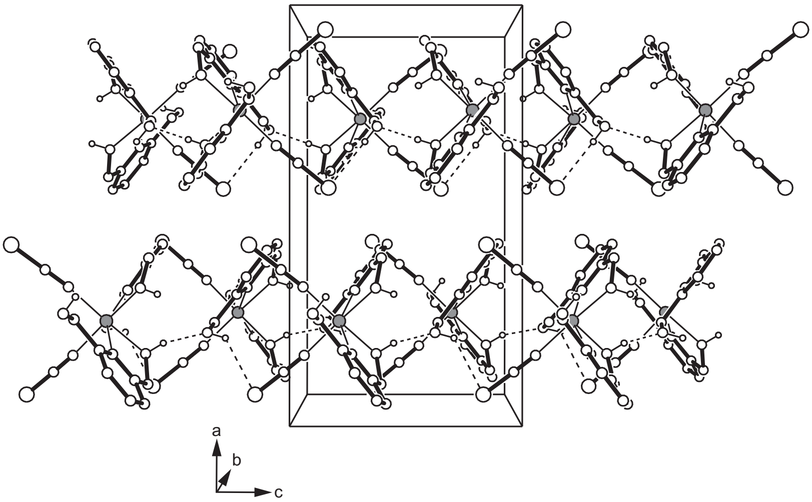

FIGURE 6 Layer structure in the crystal packing of Complex **3**. For clarity, only the hydrogens of the hydroxyl groups are shown.

cation are excluded from complexation. Instead, they are involved in contacts to the sulfur atoms (S···H 2.372, 2.628 Å) [12] and form H-bonds with O–H groups of adjacent molecules (O···H 1.811, 1.820 Å, Table V).

The presence of *quasi* 'free' functional groups as well as the restricted possibilities of the linear anions for extended intermolecular interactions leads to the formation of layer-like substructures in the crystal. The molecular arrangement within one layer is illustrated in Fig. 6. The closest distances between these layers involve sulfur atoms, which are localized in the border areas. Contacts between the layers are confined to weak interactions of the type C–H···S [12] with a distance of 2.628 Å (Table V). Mention should be made that interactions between such weak donors and acceptors as a potential stabilizing factor of crystal structures have not been the object of systematic studies [13].

Crystal Structures of $[Co(LH_2)_2](NO_3)_2$ (4) and $[Ni(LH_2)_2](NO_3)_2$ (5)

The cobalt(II) nitrate complex of dhmp **4** crystallizes in the monoclinic space group *C*2/*c*. The arrangement of donor atoms of the complex is the same as is found in **1**. However, the additional hydrogen donor in **4** and the specific coordination mode of the nitrate anions result in different crystal packing, which is shown in Fig. 7. Here, as a main structural motif, a centrosymmetric arrangement of two complex cations, connected via hydrogen bonding by two counterions (Table V), can be defined. These dimers are bridged by the second nitrate ion giving molecular double strands that run along the *a* axis. Only weak π–π-stacking interactions of the face-to-face type exist between the pyridine units of adjacent strands with centroid–centroid distances of 3.76 and 3.94 Å.

The structure of the corresponding nickel complex **5** reveals a centrosymmetric dimeric unit of complex cations with a close intermolecular distance (O3–O3′) of 2.48 Å. Analysis of the binding properties of the complex cation proved to be difficult as the position of the hydrogen atom H3′ was not available from the difference electron

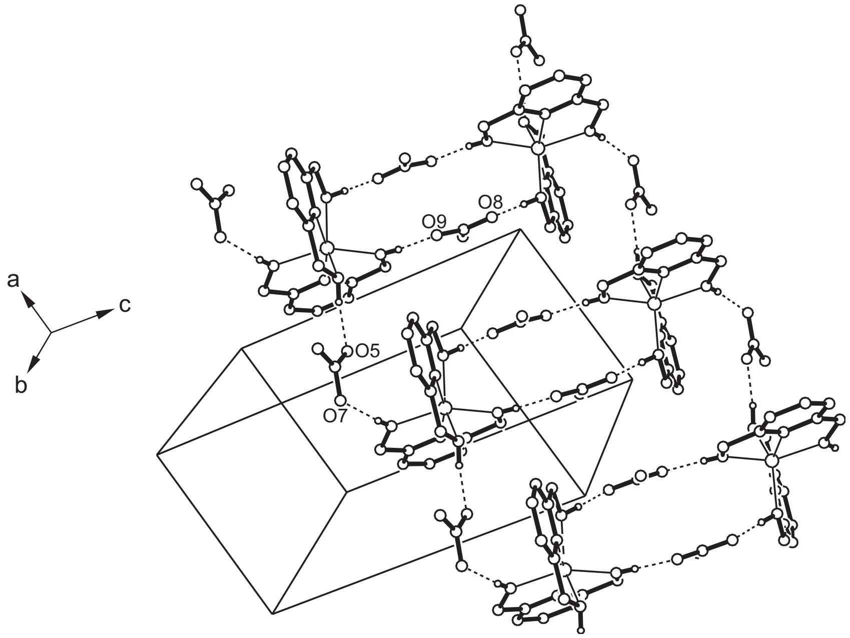

FIGURE 7 Structure of the crystal packing of Complex **4**. Only the hydrogens involved in H-bonding are shown.

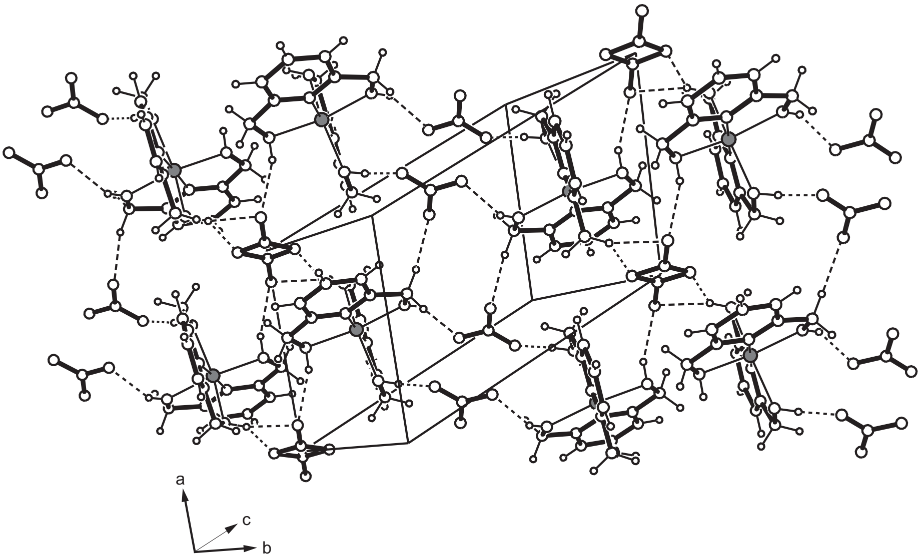

FIGURE 8 Packing structure including H-bonding system of Complex **5**. One nitrate anion is disordered.

density map. Thus, the determination of the atom position for H3′ was accomplished by geometric analysis based on reasonable hydrogen bond geometries with the disordered nitrate ion. This anion links the two complex cations of the dimer as well as the dimers themselves by formation of strong hydrogen bonds (Table V). The strong association between the ions is also reflected in the packing structure of **5** (Fig. 8).

Crystal Structures of [Co(LH$_2$)$_2$]SO$_4$ (6) and [Ni(LH$_2$)$_2$]SO$_4$ (7)

Complex **6** crystallizes in the monoclinic space group $C2/c$. The coordination sphere of the cobalt ion shows nearly equal C–N (2.052, 2.054 Å) and C–O bond lengths (2.125–2.156 Å). The deformation expressed by the N–Co–N (162. 1°) and O–Co–O angles (148.5, 148.9°) is more distinctive than that found in the other complexes (Table IV). This might be attributed to the highly cross-linked sulfate ions, of which all acceptor positions form bifurcated hydrogen bonds (Table V).

As can be seen from Table III, the complexes containing sulfate ions exhibit the highest crystal density. Hence, this exceptional position among the compounds studied is evident in the packing structure of **6** (Fig. 9). Here, the arrangement of the complex cations implies the formation of π–π aromatic stacking interactions in two directions. Along the c axis the pyridines are aligned in a strictly coplanar fashion, whereas in the b direction these units adopt a slightly tilted face-to-face orientation. The centroid–centroid distances are 4.26 and 3.87 Å, respectively.

Complex **7** (Fig. 10) formed from NiSO$_4\cdot$7H$_2$O and dhmp crystallizes in the triclinic space group P-1. Bond lengths around the nickel ion are comparable to **6** (Table IV). The dihedral angle given by the mean planes of the pyridine units (76.8°), however, suggests a stronger deformation of the complex cation than in **6** (86.3°). Although crystallizing in different crystal systems, Complexes **6** and **7** show nearly identical packing structures. A closer examination, however, reveals some differences regarding the intermolecular bonding pattern that can also be deduced from comparing hydrogen bond lengths in these structures (Table V). Moreover, the higher crystal density of **7**

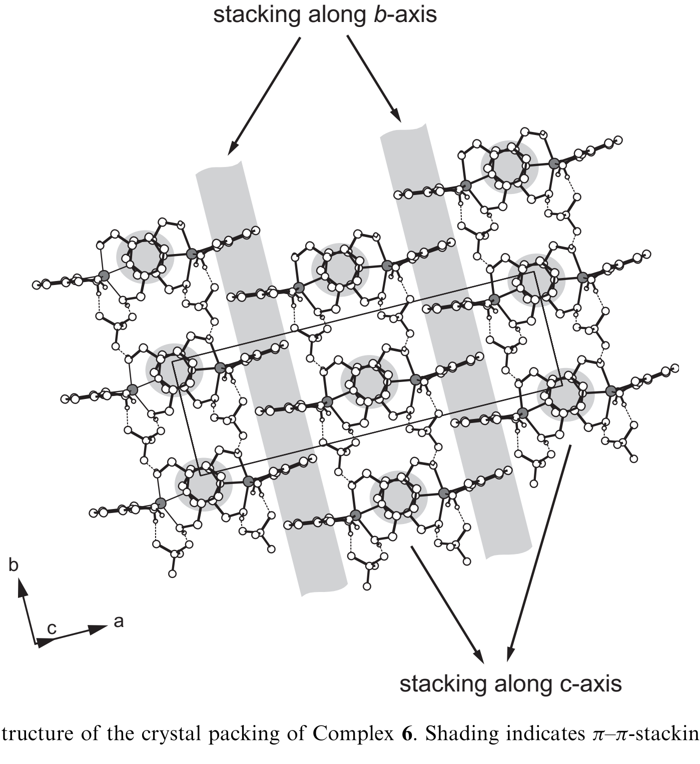

FIGURE 9 Structure of the crystal packing of Complex **6**. Shading indicates π–π-stacking interactions.

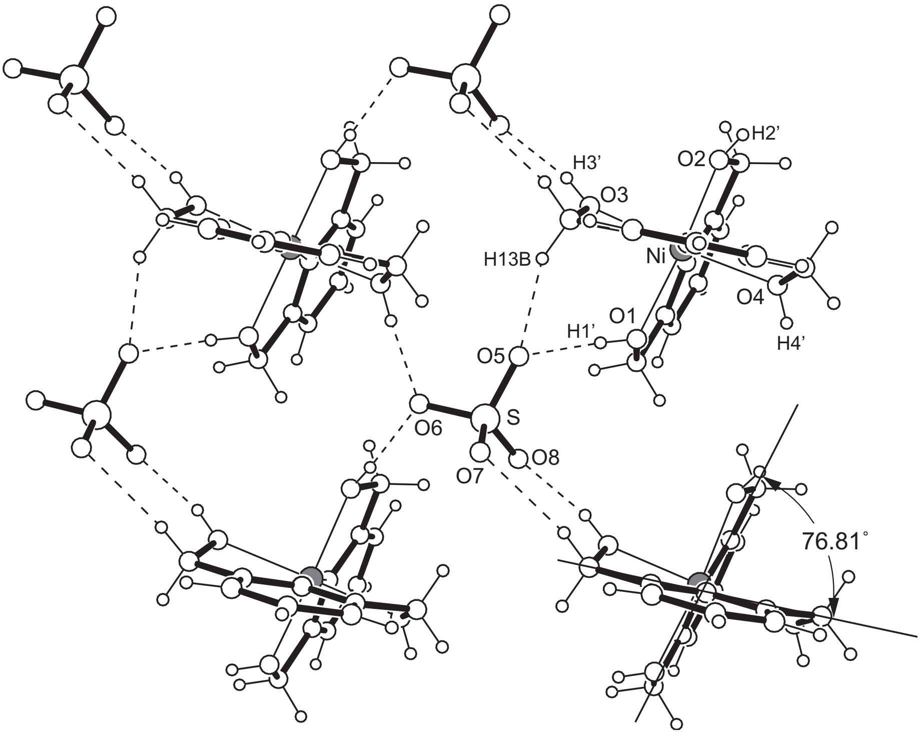

FIGURE 10 Packing structure including H-bonding system of Complex **7**.

($1.774\ \mathrm{g\,cm^{-3}}$) correlates with stronger π–π aromatic interactions, with distances of 3.58 and 4.03 Å between the arene units involved.

Crystal Structures of [Co(LH$_2$)$_2$](OTos)$_2$ (8) and [Ni(LH$_2$)$_2$](OTos)$_2$ (9)

The cobalt complex **8** and the respective nickel complex **9** crystallize in the triclinic space group *P*-1 with nearly identical cell volumes but with different lattice constants (Table III). Coordination polyhedra of the metal ions have the same configuration with nitrogens in axial positions. Also, M–O and M–N bond lengths are in the same range as related copper(II) complexes [8] and differ only slightly (Table IV).

The principles of molecular order in the structures of **1**–**7**, which are based on stacking interactions between the pyridine units, are absent in **8** as a result of the amphiphilic character of the tosylate ion. As phenyl residues of the tosylate participate in a stacked arrangement, only two of the oxygen atoms can be used for hydrogen bond formation. Consequently, two-dimensional uncongested networks with alternating cations and tosylate ions are formed that run parallel to the *ab* plane. These molecular sheets are associated by stacking interactions in which oppositely charged ions are arranged in pairs (Fig. 11).

Similar coordination behavior of the tosylate ions is also present in the nickel complex **9**. However, its packing structure is different from the cobalt complex, being characterized by the formation of linear double strands that are stabilized in a complicated manner by hydrogen bonds and aromatic interactions between phenyl and

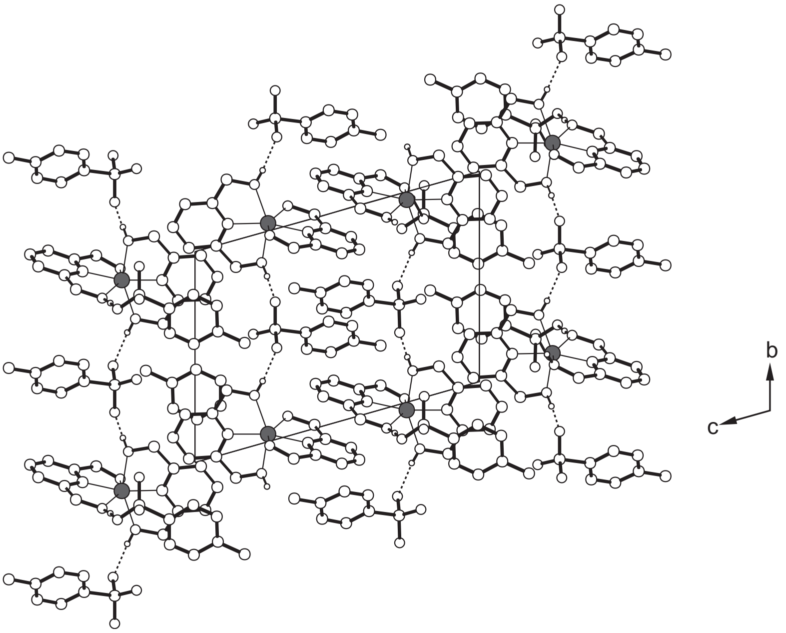

FIGURE 11 Packing structure of Complex **8**. Only the hydrogens involved in H-bonding are shown.

pyridyl residues (Fig. 12). In this arrangement, the aromatic units of the tosylate ions create hydrophobic regions that separate polar structure domains.

CONCLUSIONS

The ligand 2,6-bis(hydroxymethyl)pyridine (dhmp) was investigated with regard to complex formation with nickel and cobalt salts containing different counterions (Cl^-, SCN^-, NO_3^-, SO_3^{2-}, $OTos^-$) and this led to the isolation of nine crystalline complexes (**1**–**9**). All complexes are mononuclear species of 2 : 1 (ligand:salt) stoichiometry. Nevertheless, Complexes **1** and **2**, containing chloride, are an exception in that they are hydrated species with one, and one-half of a water molecule per formula unit, respectively; the water is not involved in metal coordination. Moreover, Complex **1** contains Co(III) instead of Co(II) as for the other cobalt complexes (**3**, **4**, **6**, **8**), indicating that oxidation occurred under the given conditions and one of the dhmp ligands is mono-deprotonated.

Irrespective of this, in all complexes except **3**, the metal ions are hexacoordinated with distorted octahedral geometry involving two nitrogens and four oxygens in the coordination sphere, in which dhmp acts as a tridentate ONO-donor ligand. In **3** the coordination sphere is formed by two nitrogens and two oxygens of dhmp, and two nitrogens of coordinated thiocyanates [13]. Here the chelating dhmp behaves as a bidentate NO-donor ligand. Except for **1**, in all complexes of structure MN_2O_4 (**2**, **4**–**9**) the basal plane is filled by the O atoms of the hydroxyl groups and pyridine nitrogens occupy axial positions; in **1**, one of the dhmp ligands is mono-deprotonated and acts as an anionic component. This gives rise to another arrangement around the

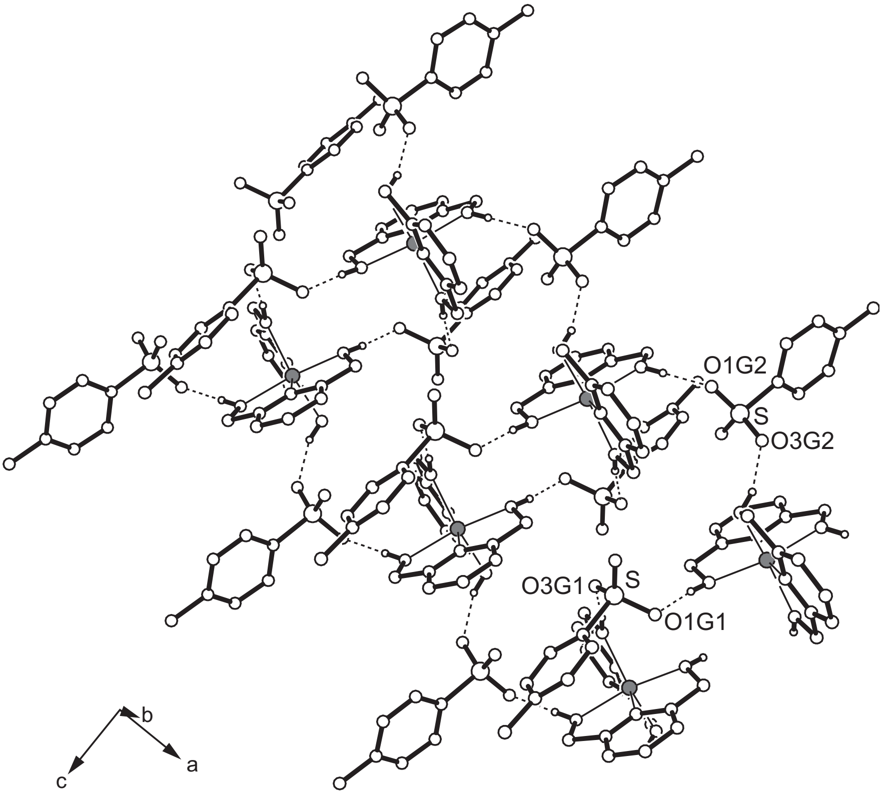

FIGURE 12 Packing structure of Complex **9** indicating the system of H-bonds.

cobalt center, in that the base is occupied by two pyridine nitrogens and two oxygens of mono-deprotonated dhmp (LH), while the OH groups of the neutral dhmp occupy axial positions. In Complex **3** also the basal plane is formed by two N and O donor atoms, but the pyridine nitrogens are apical, as in **2** and **4**–**9**.

A further common structural feature of Complexes **1**, **2** and **4**–**9** is the distorted conformation of the coordination polyhedra. In particular, the bases of the octahedra have a twisted form caused by the rigidity of the chelating ligand. Nevertheless, the bond angles N1–M–N2, O1–M–O2 and O3–M–O4 of the different complexes (Table IV) show that the coordination polyhedra of the nickel complexes **2**, **5**, **7** and **9** are more symmetrical than the cobalt complexes **1**, **4**, **6** and **8**. This can be attributed to the marked Jahn–Teller effect of Co complexes [14]. Only in Complex **3** does the specific behavior of dhmp as a bidentate ligand lead to a more regular, less strained coordination polyhedron.

In comparison with previously studied copper complexes of dhmp [8], the present cobalt and nickel complexes permit a general conclusion. If the coordination environment has the structure MN_2O_4 with the nitrogens in apical positions, an axially compressed coordination polyhedron results. On the other hand, if the O atoms are in apical positions, the octahedra are stretched in the axial direction.

Moreover, the packing modes of the complexes demonstrate significant network structures in which free binding sites of the ligand and counterions are involved to form more or less complex systems of H-bonds including weak C–H···O and O–H···S as well as stronger O–H···Cl contacts [15] (Table V). In this respect, the Co and Ni complexes are similar to the Cu complexes of dhmp [8].

In summary, dhmp has proved to be a versatile chelating ligand for the complexation of cobalt, nickel and copper [8], and thus is a promising coordination building block for the design of coordination polymers involving these and other metal ions. Of particular interest is the bidendate behavior of dhmp in Complex **3**, where free hydroxy groups are available to be used for immobilization in a polymeric matrix, as a support for catalytic reactions or for creation of new hybrid, H-bond assisted, coordination polymers [16]. Similar behavior is expected for the complexes with certain other metals such as platinum [4] or technetium [5]. Moreover, the soft sulfur atom of the thiocyanate in **3** is probably a good donor site for coordination to soft acceptors such as mercury [17], which could be used for the construction of new, mixed metal polymeric aggregates [18].

Acknowledgments

This work was supported by the German Ministry of Education and Research (BMBF-Project 'BioMon' 02110120) and the Fonds der Chemischen Industrie. We also thank Professor G. Roewer (Institute of Inorganic Chemistry) for helpful discussions and the research group of Professor Niklas (Institute of Experimental Physics) for EPR measurements.

References

[1] (a) R.J.H. Clark and C.S. Williams, *Inorg. Chem.* **4**, 350 (1965); (b) R.H. Nuttall, A.F. Cameron and D.W. Taylor, *J. Chem. Soc., A* 3103 (1971); (c) D.A. Thornton, *Coord. Chem. Rev.* **104**, 251 (1990).

[2] (a) P. Losier and M.J. Zaworotko, *Angew. Chem.* **108**, 2957; *Angew. Chem., Int. Ed. Engl.* **35**, 2779 (1996); (b) M. Fujita, *J. Synth. Org. Chem. Jpn.* **54**, 953 (1996); (c) K. Kasai, M. Aoyagi and M. Fujita, *J. Am. Chem. Soc.* **122**, 2140 (2000); (d) R. Kitaura, K. Fujimoto, S. Noro, M. Kondo and S. Kitagawa, *Angew. Chem.* **114**, 141; *Angew. Chem., Int. Ed. Engl.* **41**, 133 (2002); (e) B.F. Abrahams, B.F. Hoskins and R. Robson, *J. Am. Chem. Soc.* **113**, 3606 (1991).

[3] (a) F. Lions and K.V. Martin, *J. Am. Chem. Soc.* **79**, 2733 (1957); (b) E. Buhleier, W. Wehner and F. Vögtle, *Liebigs Ann. Chem.* **4**, 537 (1978); (c) G. Ferguson, K.E. Matthes and D. Parker, *J. Chem. Soc., Chem. Commun.* 1350 (1987); (d) Y. Couturier and C. Petitfaux, *Bull. Soc. Chim. Fr.* **129**, 335 (1992); (e) B. Nock, H.-J. Pietzsch, F. Tisato, T. Maina, P. Leibnitz, H. Spies and E. Chiotellis, *Inorg. Chim. Acta* **304**, 26 (2000).

[4] F.D. Rochon, A.L. Beauchamp and C. Bensimon, *Can. J. Chem.* **74**, 2121 (1996).

[5] F.D. Rochon, R. Melanson and P.-C. Kong, *Inorg. Chim. Acta* **254**, 303 (1997).

[6] N. Farfán and H. Höpfl, *Heteroatom Chem.* **9**, 377 (1998).

[7] M. Koman, M. Melník and J. Moncol, *Inorg. Chem. Commun.* **3**, 262 (2000).

[8] S. Winter, W. Seichte and E. Weber, *Z. Anorg. Allg. Chem.* **630**, 434 (2004).

[9] G.M. Sheldrick, *SHELXS 97, Program for Crystal Structure Solution* (University of Göttingen, Germany, 1997).

[10] G.M. Sheldrick, *SHELXL 93, Program for Crystal Structure Refinement* (University of Göttingen, Germany, 1993).

[11] L.J. Farrugia, *WinGX-Version 1.64.05* (Department of Chemistry, University of Glasgow, 2003).

[12] (a) C.M.V. Stalhandske, C.I. Stalhanske, M. Sandström and I. Persson, *Inorg. Chem.* **36**, 3167 (1997); (b) C.M.V. Stalhandske, I. Persson, M. Sandström and M. Aberg, *Inorg. Chem.* **36**, 4945 (1997).

[13] A.H. Norbury and A.I.P. Shina, *Q. Rev. Chem. Soc.* **24**, 69 (1970).

[14] J.E. Huheey, E.A. Keiter and R.L. Keiter, *Inorganic Chemistry: Principles of Structure and Reactivity*, 4th edn (Addison-Wesley, New York, 1997).

[15] G.R. Desiraju and T. Steiner, *The Weak Hydrogen Bond in Structural Chemistry and Biology*. IUCr Monographs on Crystallography, Vol. 9 (Oxford University Press, Oxford, 1999).

[16] (a) E. Weber (Ed.), *Design of Organic Solids*. Topics in Current Chemistry, Vol. 198 (Springer-Verlag, Berlin–Heidelberg, 1998); (b) G.R. Desiraju (Ed.), *Crystal Design: Structure and Function*. Perspectives in Supramolecular Chemistry, Vol. 7 (Wiley, Chichester, 2003).

[17] (a) A.L. Beachamp, L. Pozdornik and R. Rivest, *Acta Crystallogr., Sect. B* **32**, 650 (1976); (b) M.R. Udupa and B. Krebs, *Inorg. Chim. Acta* **42**, 37 (1980).

[18] I. Haiduc and F.T. Edelmann, *Supramolecular Organometallic Chemistry* (Wiley-VCH, Weinheim, 1999).